

# 3D-soliton waveguides in lithium niobate for femtosecond light pulses

V I Vlad<sup>1</sup>, A Petris<sup>1</sup>, A Bosco<sup>2</sup>, E Fazio<sup>2</sup> and M Bertolotti<sup>2</sup>

<sup>1</sup> Institute of Atomic Physics, NILPRP-Romanian Center of Excellence in Photonics, Bucharest, Romania

<sup>2</sup> Università 'La Sapienza' e INFN, Dipartimento di Energetica, Via Scarpa 16, I-00161 Roma, Italy

E-mail: [vlad@ifin.nipne.ro](mailto:vlad@ifin.nipne.ro)

Received 14 November 2005, accepted for publication 2 February 2006

Published 7 June 2006

Online at [stacks.iop.org/JOptA/8/S477](http://stacks.iop.org/JOptA/8/S477)

## Abstract

We show that efficient waveguides can be written by bright spatial solitons in the volume of lithium niobate photorefractive crystals by cw and pulsed laser beams. Using high-repetition-rate femtosecond laser pulses, an efficient formation of soliton waveguides (SWGs) is possible, after accumulating a large number of pulses, because the characteristic photorefractive build-up time is much longer than the pulse period and the efficient two-photon absorption may contribute to the solitonic confinement. These results open the possibility of writing reconfigurable single SWGs and SWG arrays (with any spatial orientation and large range of periods) and optimally guiding the femtosecond pulsed laser beams through them, creating a graded refractive-index profile matched to the spatial beam profile. Our experiments also show a small increase in pulse duration (small dispersion) in these waveguides.

**Keywords:** optical waveguides, spatial solitons, photorefractive crystals

## Introduction

Modern technologies lead to the strong development of both one-dimensional (1D) and two-dimensional (2D) optical waveguides. Three-dimensional (3D) optical waveguide technology is still under investigation.

To realize 1D and 2D waveguides, different methods have been proposed, from growing layers of thin films or channels on substrates (epitaxial growing, RF sputtering evaporation or spin-coating [1, 2]) to locally modifying the material refractive index by damaging [3] or doping the external surface (thermal diffusion from thin film [4, 5], ion exchange [6, 7], ion implantation [8, 9]). In all of these techniques, the waveguides are at the surface of the substrate.

The progress of technology is pushing optical circuitry towards the third dimension, into the substrate depth. Recently, direct laser writing of buried waveguides was demonstrated using a transversal configuration, whereby ultrafast laser pulses were focused through the lateral crystal face inside the material. At the focal point, these pulses have such a high intensity that they can cause controlled damage to the

material, which can guide the light. Recently the formation of channel waveguides 1 mm deep in the substrate has been demonstrated [10]. Direct laser writing of waveguides is clearly a more versatile technique, even though it is still affected by some limitations, mainly due to the focusing procedure and by the refractive-index profile that can be obtained by this laser treatment.

All techniques such as layer growing, in-diffusion and direct laser writing create waveguides with refractive-index profiles, which are determined by the physical fabrication process and are not yet optimized for the best propagation performances (best modal distribution, losses and dispersion).

Lithium niobate (LiNbO<sub>3</sub>—LN) is a widely used material in optical waveguides. Among all of the effects that this material offers, we shall focus our attention on the electro-optic one. It yields optical nonlinearities in LN, which are based either on the generation of a local photovoltaic electric field [11], or the generation of bound carrier populations, that can produce the screening of a uniform externally applied bias [12], or on a combination of the two [12, 13]. These processes can be used for spatial

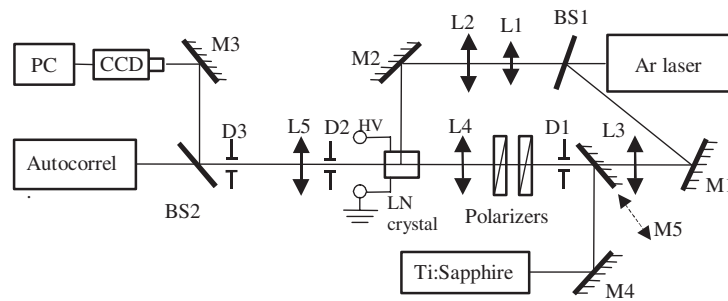


**Figure 1.** Experimental set-up for writing SWGs with a cw (argon ion laser) and to study the propagation of femtosecond laser pulses through such waveguides.

soliton propagation. Analytical predictions have been made for obtaining optical spatial solitons, either bright or dark in LN [13–15]. Experimentally dark solitons have been observed [16–18] without any external bias, in the open-circuit configuration [19]. The transition from defocusing to focusing behaviour of photovoltaic nonlinearities has been predicted and experimentally observed in the open-circuit configuration [20], opening the possibility of bright photovoltaic soliton generation in LN.

Screening-photovoltaic bright solitons were indeed observed and experimentally characterized by cw green laser beams [21]. Pulsed lasers were used to test screening solitons [22].

Spatial solitons with two-dimensional light confinement open the possibility of writing 3D optical waveguides, which have an optimum graded refractive-index profile matched to the fundamental laser mode profile and can be temporarily stored, erased, rewritten or can even be permanently fixed [23–25].

In this paper, we show good waveguiding of ultrafast laser beams in SWGs with low pulse dispersion. SWGs are written with low-power cw laser beams or using high-repetition-rate femtosecond laser pulses. In the second case, an efficient writing of SWGs is possible, after accumulating a large number of pulses, because the characteristic photorefractive build-up time is much longer than the pulse period, and the efficient two-photon absorption may contribute to the solitonic confinement. Several SWGs were induced in the volume of the same LN crystal (3D), in different positions. The SWGs show reproducible features with no perturbations of previously recorded SWGs produced by the multiple writing procedures in the same crystal. They show a controllable transversal profile in terms of their writing time, as well as a long lifetime and a low dispersion for ultrashort laser pulse propagation.

## 1. Bright SWG formation in LN with cw laser beams at 514 nm for guiding femtosecond laser pulses

We used the experimental set-up shown in figure 1 for writing SWGs in the intrinsic LN crystals and the propagation of femtosecond laser pulses through these waveguides.

In the first experiment, the laser beam from a cw argon ion laser ( $\lambda = 514$  nm), linearly polarized, with a Gaussian transversal intensity distribution, was split into two beams for signal and background. The signal beam was focused to a

diameter of about  $18 \mu\text{m}$  on the input face of the crystal of 5 mm thickness ( $\sim 5$  diffraction lengths). This beam propagated along the  $z$ -direction, orthogonally to the optical axis ( $y$ -direction). A bias voltage was applied on the LN crystal along the optical axis. The background beam, which was mutually incoherent to the signal beam, was expanded and sent along the  $x$ -direction in the crystal. The crystal was immersed in a cell with insulating oil, and placed on a stage that allowed the fine adjustment of the crystal position for optimum coupling of the probe beam to the different SWGs induced in the crystal. An imaging system was used to visualize the transversal shape of the signal beam at the input and output planes of LN crystal.

The temporal evolution of the beam shape at the output plane is shown in the figure 2(a), for a static bias  $E_0 = 35 \text{ kV cm}^{-1}$  and a ratio  $r \sim 3300$  between the intensity of the signal beam ( $I_s = 8.6 \text{ W cm}^{-2}$ , signal power  $10 \mu\text{W}$ ) and of the background beam ( $I_b = 2.6 \text{ mW cm}^{-2}$ ). The full procedure for SWGs writing is described in [26, 27].

The soliton waveguide becomes cylindrical with circular sections at  $E_0 = 35 \text{ kV cm}^{-1}$  and with a cw exposure for about 30 min (figure 2(b)). After this time, there were no noticeable changes in beam waists along the two directions. Different guiding properties can be obtained depending on the duration of the SWG writing. If cutting the voltage on the crystal when the confinement is reached on the  $y$ -direction, the soliton channel has guiding properties mainly on this direction.

The temporal stability of the induced SWGs was checked for up to 1 month by monitoring their guiding properties when coupling to waveguide, for short times, the light with the same wavelength as used for writing. No effective change of the output profile of the beam transmitted through the waveguide was observed.

Then, six SWGs were induced in the volume of an LN crystal (3D) with different recording times: WG1—15 min recording time, WG2 and WG3—30 min, WG4—60 min, WG5 and WG6—90 min, showing reproducible features, as shown in figure 2.

The propagation of ultrashort pulses through these SWGs was tested by guiding 75 fs pulses generated by a mode-locked Ti:sapphire laser (figure 3). The beam with 35 mW average power, injected into the waveguides, was polarized along the  $c$ -axis of the crystal. We compared the signal beam shape at the input with the beam shape at the output, within or outside the six different soliton waveguides.

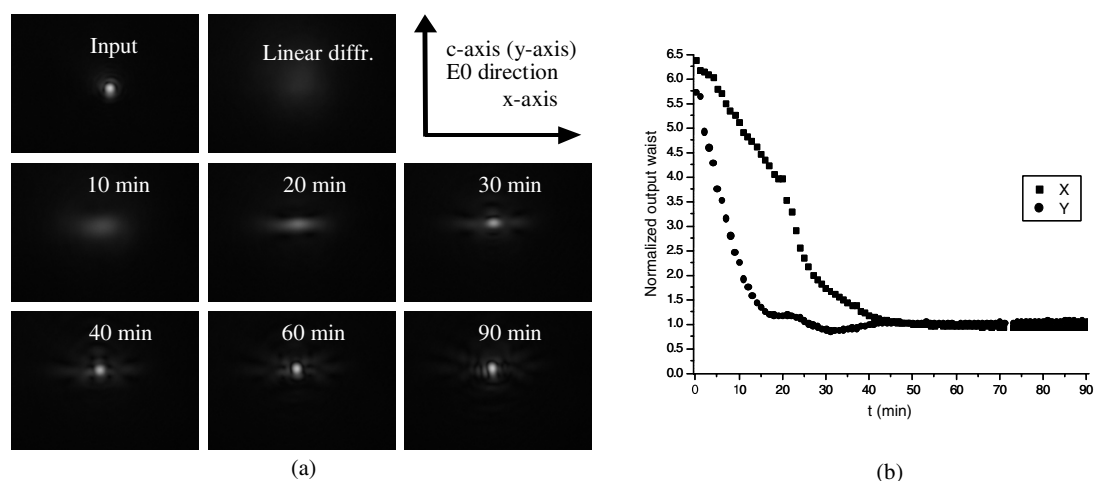


**Figure 2.** The temporal evolution of the transversal shape of the signal beam at the output of the crystal (a) and of the normalized output beam widths along the  $x$  and  $y$ -axis (b). The experimental conditions are characterized by:  $E_0 = 35 \text{ kV cm}^{-1}$ ; the intensity of the signal beam,  $I_s = 8.6 \text{ W cm}^{-2}$ , (signal power  $10 \mu\text{W}$ ) and of the background beam ( $I_b = 2.6 \text{ mW cm}^{-2}$ );  $r \sim 3300$ ; input beam diameter,  $18 \mu\text{m}$ .

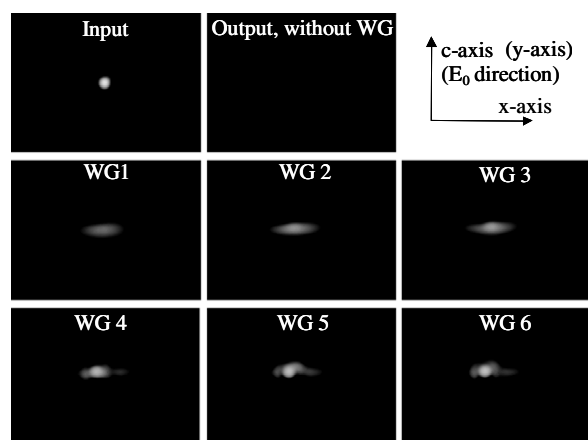


**Figure 3.** Guiding femtosecond laser beams through SWGs created by a low-power ( $10 \mu\text{W}$ ) cw argon ion laser.

We acquired the input and output beam images and observed the beam profile along its propagation through the crystal. In figure 4, the corresponding beam profiles fitted with

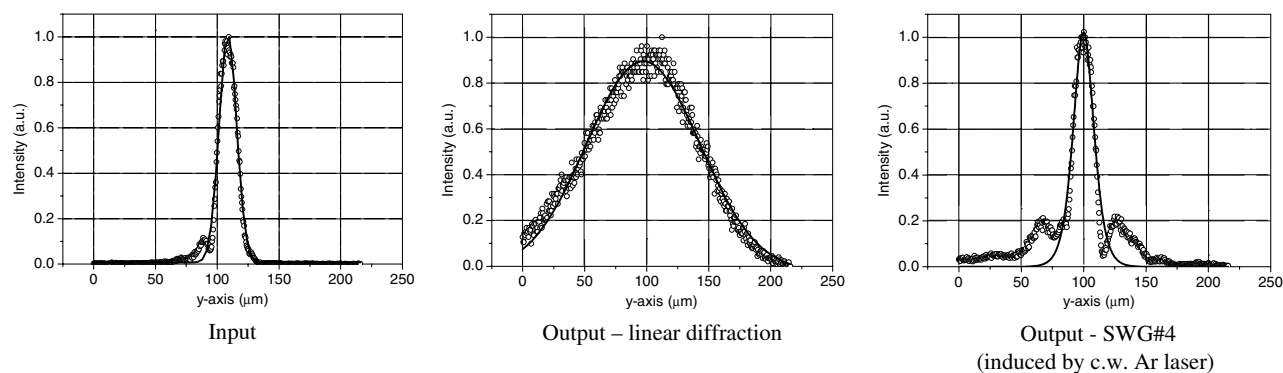


**Figure 4.** The beam profiles in the input (FWHM =  $18 \mu\text{m}$ ) and the output planes of LN crystal in the case of free propagation through the crystal (FWHM =  $96.5 \mu\text{m}$ ) and the output of SWGs (FWHM =  $19.5 \mu\text{m}$ ) induced by cw Ar laser.

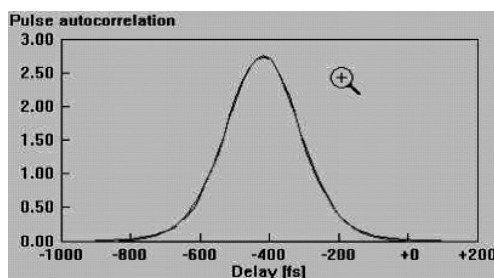
Gaussian curves (the input beam and output beam, passing through the crystal, outside waveguides) and respectively with a hyperbolic secant curve (the output beam passing through a soliton waveguide) are shown. The beam profiles conserve their widths over  $\sim 5$  diffraction lengths of propagation.

The changes in the pulse duration produced by different SWGs were also measured. For these measurements, we used an autocorrelator (FemtoScope) coupled to a PC, in the intensimetric (background free) mode of operation. The temporal profile of the fs pulses was very well fitted by a  $\text{sech}^2$  curve (figure 5). In all measurements, the crystal remained immersed in the cell with insulating oil. The pulse durations, for these different paths, were obtained by averaging 20 different measurements done with the autocorrelator (and calculating the standard deviation). In each measurement, 150 acquisition sequences (each of them of 40 scans) were averaged by the FemtoScope.

In table 1, the output pulse durations for: (a) a fs-beam passing through the cell with oil (near to the crystal), (b) a fs-beam passing through the crystal in a region where a waveguide is not induced and (c) a fs-beam passing through the six different waveguides induced in the crystal (previously mentioned) are compared.

**Table 1.** Average pulse duration of fs beam after passing through the cell with oil only and through LN crystal in regions without and with induced waveguides (WG1–6).

Material	Oil	Crystal	WG1 15 min	WG2 30 min	WG3 30 min	WG4 60 min	WG5 90 min	WG6 90 min
Average pulse duration (fs)	112.4	164.1	164.9	166.0	165.8	169.4	168.2	169.2
Standard deviation of pulse duration (fs)	1.2	2.1	1.8	2.4	1.9	2.5	1.7	1.5

**Figure 5.** The pulse duration at SWG output, 162.2 fs, measured with an autocorrelator, in the background free mode of operation. The temporal profile of fs pulses was very well fitted by a  $\text{sech}^2$  curve.

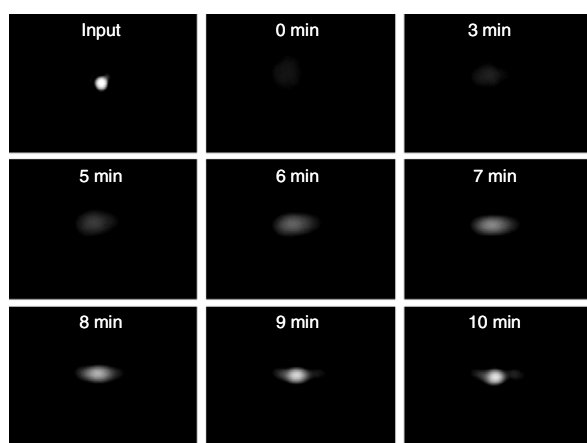
In comparison with the large change of the pulse duration induced by the cell with oil and the crystal, only a very small increase in the pulse duration is produced by the soliton waveguides ( $\sim 1$  fs  $\text{mm}^{-1}$ ).

## 2. SWG formation in LN with femtosecond pulsed laser beams at the wavelength of 800 nm for guiding femtosecond laser pulses

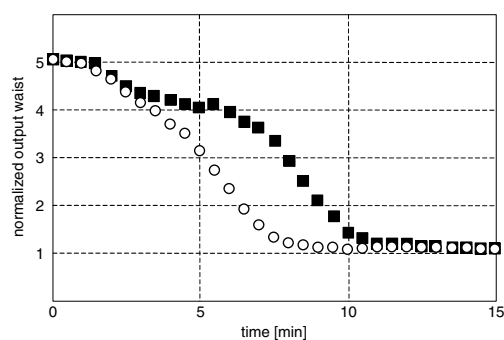
To study SWG formation in LN with femtosecond pulsed laser beams, we replaced, in the experimental set-up shown in the figure 1, the Ar laser with a Ti:sapphire laser, delivering pulses of 75 fs, with a repetition rate of 78 MHz, at wavelength 800 nm, which provides the signal beam. The signal is focused down to about 18  $\mu\text{m}$  (FWHM) on the input (100) face of

the crystal and has the average power of 16 mW. The green background, illuminating the (010) crystal face, is provided by a cw argon-ion laser beam, at 514 nm or alternatively, by a LED. The background beam was set in order to give a uniform illumination of  $\sim 10$  mW  $\text{cm}^{-2}$ . The LN crystal (5 mm long) was electrically biased at 35 kV  $\text{cm}^{-1}$  along its optical-axis direction ([001] crystallographic direction). The change of the pulse duration inside the LN crystal was  $\sim 10$  fs  $\text{mm}^{-1}$ ; nonlinear dispersion was negligible. The input and output crystal planes are imaged on a CCD sensor of a computer interfaced camera.

The dynamics of the Ti:sapphire laser beam propagating inside the LN crystal, with the background illumination, is shown in figure 6, where the beam profile at the input face is shown for comparison. The linear diffraction inside the crystal is evident at the initial experimental time (0 min), for which both the bias and the beam were turned on. In such a case, the self-focusing was very efficient from the first minutes, firstly along the vertical direction, which corresponds to the optical axis of the crystal. This process was already observed in the cw regime [21], where the beam confinement along this axis was faster than along the other one. As shown in figure 6, the bright soliton size (18  $\mu\text{m}$ , FWHM) along the vertical axis was reached after 8 min, whereas along the horizontal axis, it was slower, reaching the same size after about 11 min. As previously reported [21], solitons with circular sections (single-mode fibre type) are also obtained in this experiment with LN; however due to the high light intensity (1.1 GW  $\text{cm}^{-2}$ ) and the high bias field applied



(a)



(b)

**Figure 6.** (a) The dynamics of SWGs induced with a femtosecond pulsed laser beam (800 nm,  $I_s = 1.1$  GW  $\text{cm}^{-2}$ ) with cw green background (514 nm,  $I_b = 10$  mW  $\text{cm}^{-2}$ ). (b) The temporal evolution of the bright soliton formation (output waist normalized to the input one) along the y-axis (optical axis of the crystal) (open circles) and x-axis (closed squares) of the beam profile.

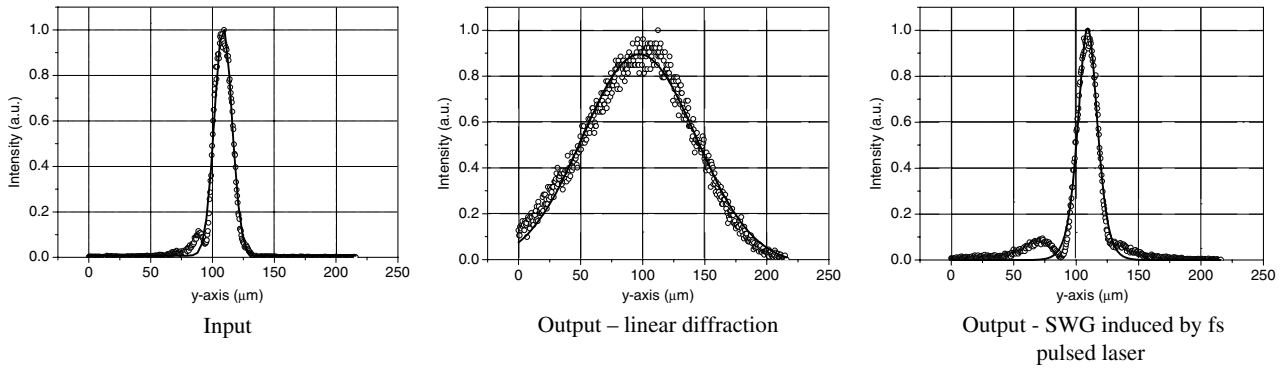


**Figure 7.** The beam profiles in the input (FWHM = 18  $\mu\text{m}$ ) and the output planes of LN crystal in the case of free propagation through the crystal (FWHM = 96.5  $\mu\text{m}$ ) and for SWGs induced by femto-laser with a cw green background (FWHM = 18  $\mu\text{m}$ ).

(35  $\text{kV cm}^{-1}$ ), a bending of the beam was observed, as high as 40–50  $\mu\text{m}$ , which slightly distorts the beam.

Soliton formation in LN crystal, which shows low sensitivity in the red spectral domain, could rely on two main processes: direct transitions from shallow traps [1] and two-photon-absorption (TPA) [28–32] from deep levels. Both of these processes, as previously reported, can occur even in ‘intrinsic’ LN. TPA can even overpass the linear absorption for high intensities: in our case, the linear absorption was as high as 0.06  $\text{cm}^{-1}$ , while the TPA, at 1  $\text{GW cm}^{-2}$ , was 0.25  $\text{cm}^{-1}$ , i.e. four times larger.

A weak green background (few  $\text{mW cm}^{-2}$ ) cannot favour the absorption in (infra-) red (at 800 nm), which was observed [22, 33] at much higher green light intensities (and in doped LN only). It creates, in the LN crystal, a (spatial) uniform distribution of ionized traps. These traps strongly reduce the average ‘free’-path of the carriers excited by the signal femtosecond pulsed beam (800 nm). The resulting carrier distribution will be concentrated in a volume approximately limited by the signal beam boundary, where a strong drift field can overpass the photovoltaic field. The resulting screening field induces the light self-trapping and possible formation of bright solitons (figure 6).

The propagation of femtosecond laser pulses through self-written SWGs (figure 7) shows a pulse evolution, which is similar to that observed in cw-produced SWGs (see figure 4 and table 1). Moreover, one can observe a smaller perturbation of the beam shape at the output of the SWG in LN crystal, which can be explained by the wavelength matching in this case.

When the green background illumination is switched off and the same external electric field is applied to the LN crystal, the signal beam (at 800 nm) cannot be confined into a bright soliton for the exposure times, which were comparable or longer than those used in the previous case (figure 8). However, dark solitons may occur in this case, as was previously predicted and observed.

### 3. Conclusions

Optical bright solitons open an all-optical and performing technology for writing SWGs in the volume of nonlinear optical materials commonly used in the photonics industry, such as LN. SWGs in LN are characterized by optimum matching of their refractive-index profile to the fundamental

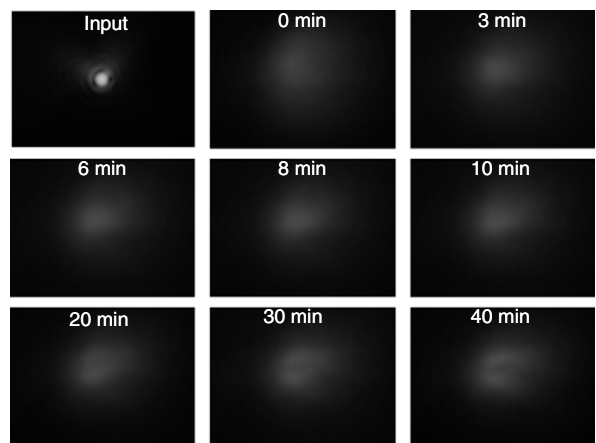


**Figure 8.** The output signal beam when the green background illumination is switched off and the same external electric field is applied to the LN crystal, for different exposure times.

laser mode profile, and open the possibility of long lifetime, erasing and fixing as well as (3D) multiplexing in the crystal volume.

We have created SWGs in nominally undoped LN crystals with low-power cw green lasers and with high-repetition-rate femtosecond laser pulses, at 800 nm, assisted by a green background and an external electrical field. The SWG formation was observed after accumulation of a large number of pulses, because the characteristic photorefractive build-up time is much longer than the pulse period and the efficient two-photon absorption may contribute to the solitonic confinement. The background illumination decreases the average-free-path of the free carriers, making the screening effect dominant over the photovoltaic one.

They show a controllable transversal profile in terms of their writing time, as well as a long lifetime and a low dispersion for ultrashort laser pulse propagation. SWGs and SWG arrays can be used in efficient reconfigurable optical interconnections.

### Acknowledgments

This work has been supported by the Bilateral Collaboration Agreement in R&D between Italy and Romania, the EU-IST-2-

511616 NoE 'PHOREMOST', the national projects CEx-D11-26 and the CNCSIS Grant No 1141.

## References

- [1] Prokhorov A M, Kuz'minov Y S and Khachaturyan O A 1997 *Ferroelectrics Thin-film Waveguides in Integrated Optics and Optoelectronics* (Cambridge: Cambridge International Science Publishing)
- [2] Wong K K 2002 *Properties of Lithium Niobate, Lithium Tantalate and Potassium Titanil Phosphate* (London: IEEE)
- [3] Bentini G G, Bianconi M, Chiarini M, Corra L, Sada C, Mazzoldi P, Argiolas N, Bazzan M and Guzzi R 2002 *J. Appl. Phys.* **92** 6477
- [4] Korotky S K and Alferness R C 1987 *Integrated Optical Circuits and Components* ed L D Hutcheson (New York: Dekker) chapter 6
- [5] Schmidt R V and Kaminov I P 1974 *Appl. Phys. Lett.* **25** 458
- [6] Wong K K 1989 *Properties of Lithium Niobate* (London: INSPEC, The Institution of Electric Engineers) chapter 8
- [7] Korkishko Y N and Fedorov V A 1996 *IEEE J. Sel. Top. Quantum Electron.* **2** 187
- [8] Townsend P D 1992 *Nucl. Instrum. Methods B* **65** 243
- [9] Townsend P D 1998 *Vacuum* **51** 301
- [10] Valdivia C, Wei X M, Coric D and Herman P R 2003 *CLEO Conf. Digest Paper CWI4 (Baltimore)*
- [11] Glass A M, Von der Linde D and Negran T J 1974 *Appl. Phys. Lett.* **25** 233
- [12] Glass A M 1978 *Opt. Eng.* **17** 11
- [13] Keqing L, Yanpeng Z, Tiantong T and Xun H 2001 *J. Opt. A: Pure Appl. Opt.* **3** 262
- [14] Valley G C, Segev M, Crosignani B, Yariv A, Fejer M M and Bashaw M C 1994 *Phys. Rev. A* **50** R4457
- [15] Chun-Feng H, Bin L, Xiu-Dong S, Yong-Yuan J and Ke-Bin X 2001 *Chin. Phys.* **10** 310
- [16] Taya M, Bashaw M C, Fejer M M, Segev M and Valley G C 1995 *Phys. Rev. A* **52** 3095
- [17] Chen Z, Segev M, Wilson D W, Muller R and Maker P D 1997 *Phys. Rev. Lett.* **78** 2948
- [18] Couton G, Maillotte H, Giust R and Chauvet M 2003 *Electron. Lett.* **39** 286
- [19] Chauvet M 2003 *J. Opt. Soc. Am. B* **20** 2515
- [20] Anastassiou C, Shih M, Mitchell M, Chen Z and Segev M 1998 *Opt. Lett.* **23** 924
- [21] Fazio E, Renzi F, Rinaldi R, Bertolotti M, Chauvet M, Ramadan W, Petris A and Vlad V I 2004 *Appl. Phys. Lett.* **85** 2193
- [22] Fressengeas N, Wolfensberger D, Maufoy J and Kugel G 1999 *J. Appl. Phys.* **85** 2062
- [23] Pette J and Denz C 2001 *Opt. Commun.* **188** 55
- [24] Couton G, Maillotte H, Giust R and Chauvet M 2003 *Electron. Lett.* **39** 286-7
- [25] Klotz M, Meng H, Salamo G and Montgomery S R 1999 *Opt. Lett.* **24** 77-9
- [26] Fazio E, Ramadan W, Petris A, Chauvet M, Vlad V I and Bertolotti M 2005 *Appl. Surf. Sci.* **248** 97
- [27] Vlad V I, Fazio E, Bertolotti M, Bosco A and Petris A 2005 *Appl. Surf. Sci.* **248** 484
- [28] Von der Linde D, Glass A M and Rodgers K F 1974 *Appl. Phys. Lett.* **25** 155
- [29] Von der Linde D, Glass A M and Rodgers K F 1976 *J. Appl. Phys.* **47** 217
- [30] Kurz H and Von der Linde D 1978 *Ferroelectrics* **21** 621
- [31] Li H, Zhou F, Zhang X and Ji W 1997 *Appl. Phys. B* **64** 659
- [32] Bai Y S and Kachru R 1997 *Phys. Rev. Lett.* **78** 2944-7
- [33] Furukawa Y, Kitamura K, Alexandrovski A, Route R K, Fejer M M and Foulon G 2001 *Appl. Phys. Lett.* **78** 1970